OPTIMIZATION TECHNIQUES FOR VEHICLE DYNAMICS MODELING

Ognian NAKOV, Dessislava PETROVA
Technical University of Sofia, Bulgaria

Abstract. This paper covers the dynamic modeling of the vehicle. The basic mathematical modeling of the vehicle's non-linear lateral and roll dynamics are covered. Assumptions are made in order to linearize the model. This non-linear vehicle model uses the non-linear Pacejka tire model. The vehicle model is used for development of autonomous control method, which is optimized for parallel execution.

Key words: vehicle modeling, linearization, parallel optimization, speed up

1. Introduction

Ground vehicles have become an almost essential part of modern life where they are depended upon daily to provide services such as transportation for people and/or cargo. For this reason, much research has been devoted to the overall advancement of ground vehicle technology. Modern science has allowed for the production of ground vehicles that can operate autonomously or semi-autonomously saving both time and money. Even the military has come to rely on intelligent unmanned vehicles for performing routine and/or potentially dangerous tasks. Safety is undoubtedly a major source of motivation behind the increasing performance demands of manned ground vehicles. Steer / brake / throttle-by-wire technology has allowed for passenger vehicle safety systems such as driver assisted automated lane keeping [1] and stability control systems [2] to become realizable.

2. Vehicle Modeling

The vehicle schematic shown in figure 1 is a simple diagram of a four wheel vehicle in the lateral and longitudinal planes. In order to simplify the lateral dynamics, the longitudinal dynamics, including drive force and rolling resistance, were neglected. Additionally, the front and rear track widths (t) are assumed to be equal. As seen in Figure 1, the sideslip (β) of the vehicle is the difference between the velocity heading (v) and the true heading of the vehicle (ψ). The yaw rate (r) is the angular velocity of the vehicle about the center of gravity. The lateral forces (Fy) are shown for both the inner and outer tires as well as the front and rear tires of the vehicle.

In the figure 1, the lateral dynamics of the vehicle are derived by summing the forces and the moments about the center of gravity of the vehicle as shown in relations (1).

$$\sum F_y = m \cdot a_y = (F_{yor} + F_{yir}) + (F_{yof} + F_{yif}) \cdot \cos(\delta)$$

$$\sum M_{cg} = I_z \cdot \ddot{\psi} = -b \cdot (F_{yor} + F_{yir}) + a \cdot [(F_{yof} + F_{yif}) \cdot \cos(\delta)] + \frac{t}{2} \cdot [(F_{yof} + F_{yif}) \cdot \sin(\delta)] \quad (1)$$

where

$$a_y = (V_r + \dot{V}_y) = (V_r + \dot{V} \cdot \sin(\beta) + V \cdot \dot{\beta} \cdot \cos(\beta))$$

$$\ddot{\psi} = \dot{r}$$

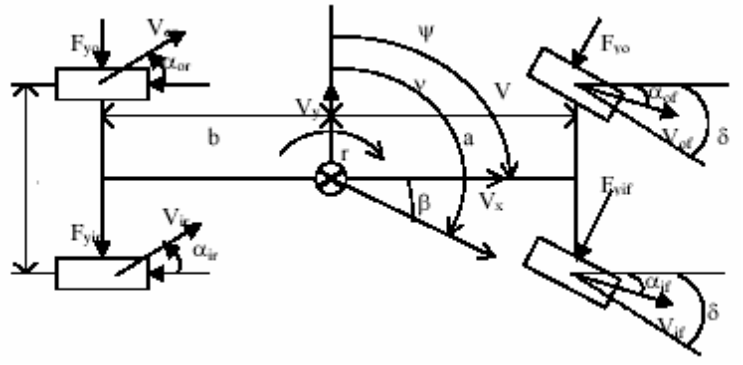

Figure 1. Wheel Vehicle Schematic Showing the Full Lateral Dynamics of a Vehicle

By solving the above equations for β and *r*, the equations of motion for the vehicles lateral dynamics can be found and are shown in equation (2).

$$\dot{\beta} = \frac{(F_{yor} + F_{yir}) + (F_{yof} + F_{yif}) \cdot \cos(\delta)}{m \cdot V \cdot \cos(\beta)} - r - \frac{\dot{V} \cdot \tan(\beta)}{V}$$
$$\dot{r} = \frac{-b \cdot (F_{yor} + F_{yir}) + a \cdot [(F_{yof} + F_{yif}) \cdot \cos(\delta)] + \frac{t}{2} \cdot [(F_{yof} + F_{yif}) \cdot \sin(\delta)]}{I_z} \quad (2)$$

The tire slip angle (α), as seen in figure 1, is the difference between the tire's longitudinal axis and the tire's velocity vector. The tire velocity vector can be found by knowing the vehicle's velocity (at the center of gravity) and yaw rate. The direction or heading of the rear tire is the same as the vehicle heading, while the heading of the front tires must include the steer angle. The equation of the tire slip angles for all four tires is given in equation (3).

$$\alpha_{if} = \tan^{-1}\left(\frac{V \cdot \sin(\beta) + a \cdot r}{V \cdot \cos(\beta) - \frac{t}{2} \cdot r}\right) - \delta$$
$$\alpha_{of} = \tan^{-1}\left(\frac{V \cdot \sin(\beta) + a \cdot r}{V \cdot \cos(\beta) + \frac{t}{2} \cdot r}\right) - \delta$$
$$\alpha_{ir} = \tan^{-1}\left(\frac{V \cdot \sin(\beta) - b \cdot r}{V \cdot \cos(\beta) - \frac{t}{2} \cdot r}\right) \quad (3)$$
$$\alpha_{or} = \tan^{-1}\left(\frac{V \cdot \sin(\beta) + a \cdot r}{V \cdot \cos(\beta) + \frac{t}{2} \cdot r}\right)$$

The roll angle (ϕ) of the vehicle is the amount of rotation of the vehicles sprung mass about its roll axis. In reality, the roll center of the vehicle does not remain constant, however in this case a stationary roll center is assumed in order to simplify the model. The roll dynamics of the vehicle are formed by separating the sprung mass and the unsprung mass at the roll center as shown in figure 2.

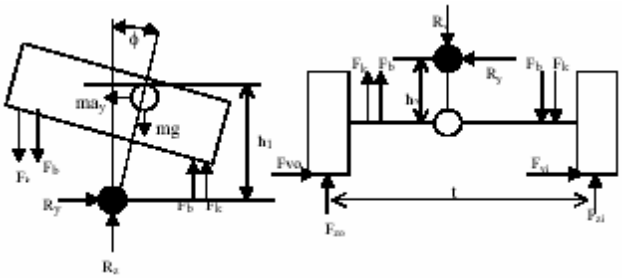

Figure 2. Free body diagram of the roll dynamics for the sprung and un-sprung mass

The equation of motion for the roll dynamics are formed by treating the system as a simple spring-mass-damper system. The equation of motion is derived by summing moments about the roll center of the vehicle for the sprung mass is given in equation (4). The moments can be summed around the roll center if a lateral centripetal force is added to the center of gravity [3].

$$\Sigma M_{rc} = I_x \cdot \ddot{\phi} + k \cdot \phi + b \cdot \dot{\phi} = \\ = -m \cdot a_y \cdot h_1 \cdot \cos\phi + m \cdot g \cdot h_1 \cdot \sin\phi \quad (4)$$

Equation (4) can be rearranged which leads to the equation for the non-linear roll dynamics of the vehicle as seen in equation (5).

$$\ddot{\phi} = \frac{-k\phi - b\dot{\phi} - ma_y h_1 \cos\phi + mgh_1 \sin\phi}{I_x} \quad (5)$$

In the above equation (*k*) is the spring stiffness, (*b*) is the damping stiffness, (h_1) is the difference between the center of gravity height and the roll center height, and (I_x) is the mass moment of inertia about the longitudinal axis. The expression for the change in vertical forces, or weight transfer, at the tires can be found by summing the moments about the roll center for the un-sprung mass for both the front and rear of the vehicle. The weight transfer, in steady state, can be found by assuming the roll is equal to zero.

The total vertical force at each wheel of the vehicle can be calculated by simply adding the weight transfer to the static weight of each tire. The equations for the total weight of all four tires is shown in equation (6).

$$F_{zif} = \frac{W_f}{2} + \Delta F_{zf} \qquad F_{zof} = \frac{W_f}{2} + \Delta F_{zf}$$
$$F_{zir} = \frac{W_r}{2} + \Delta F_{zr} \qquad F_{zor} = \frac{W_r}{2} + \Delta F_{zr} \quad (6)$$

The vertical forces and the tire slip angles can be used in order to find the total lateral force at each tire given the tire model. One popular tire model for determining the lateral tire force as a function of slip angle is the Pacejka "magic" tire

model [4]. In this method, tire parameters, that are usually unknown, are used to calculate the lateral forces of the tire. For small slip angles the force profile can be defined by a linear region and also the peak force does not increase proportionally to the vertical force (*Fz*). In the linear area of the tire curve, the slope of the line is known as the tire cornering stiffness (C_α). In the linear region of the tire curve the forces can be calculated as seen in equation (7).

$$\begin{aligned} F_{yf} &= -C_{\alpha f}\alpha_f \\ F_{yr} &= -C_{\alpha r}\alpha_r \end{aligned} \tag{7}$$

3. Linearization of the vehicle model

Some assumptions about the non-linear model of the vehicle can be made in order to linearize and simplify the model [5]. One approximation used is to neglect weight transfer. This assumption causes the vertical forces at the tires to be equal to the static weights, which are the same on the left and right side of the vehicle. The next assumption made is that the tire slip angles (α) are the same on the inner and outer sides of the vehicle. This assumption is valid if V >> tr / 2 as seen in equation (3). Also, the inner and outer tires are assumed to be the same. Assuming the same inner and outer tires results in the tire cornering stiffness (Cα) being the same for the inner and outer tires of the vehicle. Assuming no weight transfer, the same tire cornering stiffness (for the inner and outer tires), and the same tire slip angles (for the inner and outer tires) results in the lateral forces being equal for both the inner and the outer tire. Additionally, the vehicle's forward velocity is assumed to be constant in order to remove the acceleration term from the equations of motion. Finally, the small angle approximation is used in order to remove the trigametric terms from the equations of motion. These assumptions simplify the vehicle model to what is commonly known as the bicycle model. It is known as the bicycle model because the inner and outer dynamics are approximated as equal and therefore collapsed into two wheels.

The equations of motion for the lateral dynamics of the simplified model are found the same way as the non-linear model (i.e. by summing the forces and moments around the center of gravity). This leads to the equation of motion for the bicycle model shown below in Equation (8).

$$\begin{aligned} &\sum F_y = F_{yr} + F_{yr} = m \cdot a_y = m \cdot (V \cdot \dot{\beta} + v \cdot r) \\ &\sum M_y = a \cdot F_{yf} - b \cdot F_{yf} = I_z \cdot \dot{r} \end{aligned}$$

where

$$\begin{aligned} F_{yf} &= C_{\alpha f} \cdot \alpha_f \approx C_{\alpha f} \cdot \left(\beta + \frac{a \cdot r}{V} - \delta \right) \\ F_{yr} &= C_{\alpha r} \cdot \alpha_r \approx C_{\alpha r} \cdot \left(\beta - \frac{b \cdot r}{V} \right) \end{aligned} \tag{8}$$

The above linear equations of motion can be rewritten in the state space form show in equation (9)

$$\begin{aligned} \dot{x} &= A \cdot x + B \cdot u \\ y &= C \cdot x \end{aligned} \tag{9}$$

where x = state; y = measurements; u = input; A = state matrix; B = input matrix; C = output matrix.

The state space equations for the lateral dynamics can be seen in equation (10).

$$\begin{bmatrix} \dot{\beta} \\ \dot{r} \end{bmatrix} = \begin{bmatrix} \dfrac{-C_{\alpha f} - C_{\alpha r}}{mV} & \dfrac{-a \cdot C_{\alpha f} + b \cdot C_{\alpha r}}{mV^2} - 1 \\ \dfrac{-a \cdot C_{\alpha f} + b \cdot C_{\alpha r}}{I_z} & \dfrac{a^2 \cdot C_{\alpha f} + b^2 \cdot C_{\alpha r}}{I_z \cdot V} \end{bmatrix} \cdot \begin{bmatrix} \beta \\ r \end{bmatrix} + \begin{bmatrix} \dfrac{C_{\alpha f}}{m \cdot V} \\ \dfrac{a \cdot C_{\alpha f}}{I_z} \end{bmatrix} \cdot \delta \tag{10}$$

The equations for steady state yaw rate and steady state sideslip are given in equation (11). Steady state yaw rate and sideslip are dominated by the weight split and the tire cornering stiffness.

$$\begin{aligned} r_{ss} &= \frac{V}{L + V^2 \cdot K_{us}} \delta \\ \beta_{ss} &= \frac{b \cdot r}{V} - \frac{m_r \cdot V_r}{C_{\alpha f}} \end{aligned} \tag{11}$$

where

$$K_{us} = \frac{W_f}{C_{\alpha f}} - \frac{W_r}{C_{\alpha r}}$$

The understeer gradient (K_{us}) defines whether the vehicle is understeer ($K_{us} < 0$), oversteer ($K_{us} > 0$), or neutral steer ($K_{us} = 0$). The vehicle's understeer characteristics determine the change in steer angle required to hold a steady state turn as velocity increases [3].

The non-linear roll model seen in Equation (5) can be linearized by assuming small angles to remove the trigametric terms. The linearized roll equations can then be placed into the state space representation as shown in equation (12).

$$\begin{bmatrix} \dot{\phi} \\ \ddot{\phi} \end{bmatrix} = \begin{bmatrix} 0 & 1 \\ m \cdot g \cdot h_1 - k & -b \end{bmatrix} \cdot \begin{bmatrix} \phi \\ \dot{\phi} \end{bmatrix} + \begin{bmatrix} 0 \\ -m \cdot h_1 \end{bmatrix} \cdot a_y \qquad (12)$$

Since lateral acceleration consists of pure lateral acceleration plus the centripetal acceleration, it can be written as a function the derivate of sideslip and the yaw rate. By substituting the lateral acceleration in terms of the derivative of sideslip and yaw rate, the yaw and roll state space models can be coupled together as given below in equation (13).

$$\begin{bmatrix} \dot{\beta} \\ \dot{r} \\ \dot{\phi} \\ \ddot{\phi} \end{bmatrix} = \begin{bmatrix} \frac{-C_{\alpha f} - C_{\alpha r}}{m \cdot V} & \frac{-a \cdot C_{\alpha f} + b \cdot C_{\alpha r}}{m \cdot V^2} - 1 & 0 & 0 \\ \frac{-a \cdot C_{\alpha f} + b \cdot C_{\alpha r}}{I_z} & \frac{a^2 \cdot C_{\alpha f} + b^2 \cdot C_{\alpha r}}{I_z V} & 0 & 0 \\ 0 & 0 & 1 & 0 \\ \frac{-C_{\alpha f} - C_{\alpha r}}{m} & \frac{-a \cdot C_{\alpha f} + b \cdot C_{\alpha r}}{m \cdot V} & m \cdot g \cdot h_1 - k & -b \end{bmatrix} \cdot \begin{bmatrix} \beta \\ r \\ \phi \\ \dot{\phi} \end{bmatrix} + \begin{bmatrix} \frac{C_{\alpha f}}{m \cdot V} \\ \frac{a \cdot C_{\alpha f}}{I_z} \\ 0 \\ \frac{C_{\alpha f}}{m} \end{bmatrix} \cdot \delta \qquad (13)$$

4. Parallel optimization of the vehicle model

The presented vehicle model is a start point for development of a method for autonomous control. As you know each real-time system requires to be optimized in respect of calculation process. That is way a functional decomposition is realized for suggested method for autonomous vehicle control. As result two tasks are obtained: task 1 and task 2, which require sequentional execution, because task 2 has to wait execution of task 1. Also for task 1 data decomposition is realized. The decomposition can be seen in figure 3.

The data decomposition of task 1 is presented with task graph shown in figure 3. The graph edges correspond to the data dependences, which define that calculation of one value requires calculation of another value. The graph nodes are marked with the result of each subtask execution.

Amdahl's law states that potential program speedup is defined by the fraction of code that can be parallelized [6]. By means of the realized decomposition and after analysis of the source code

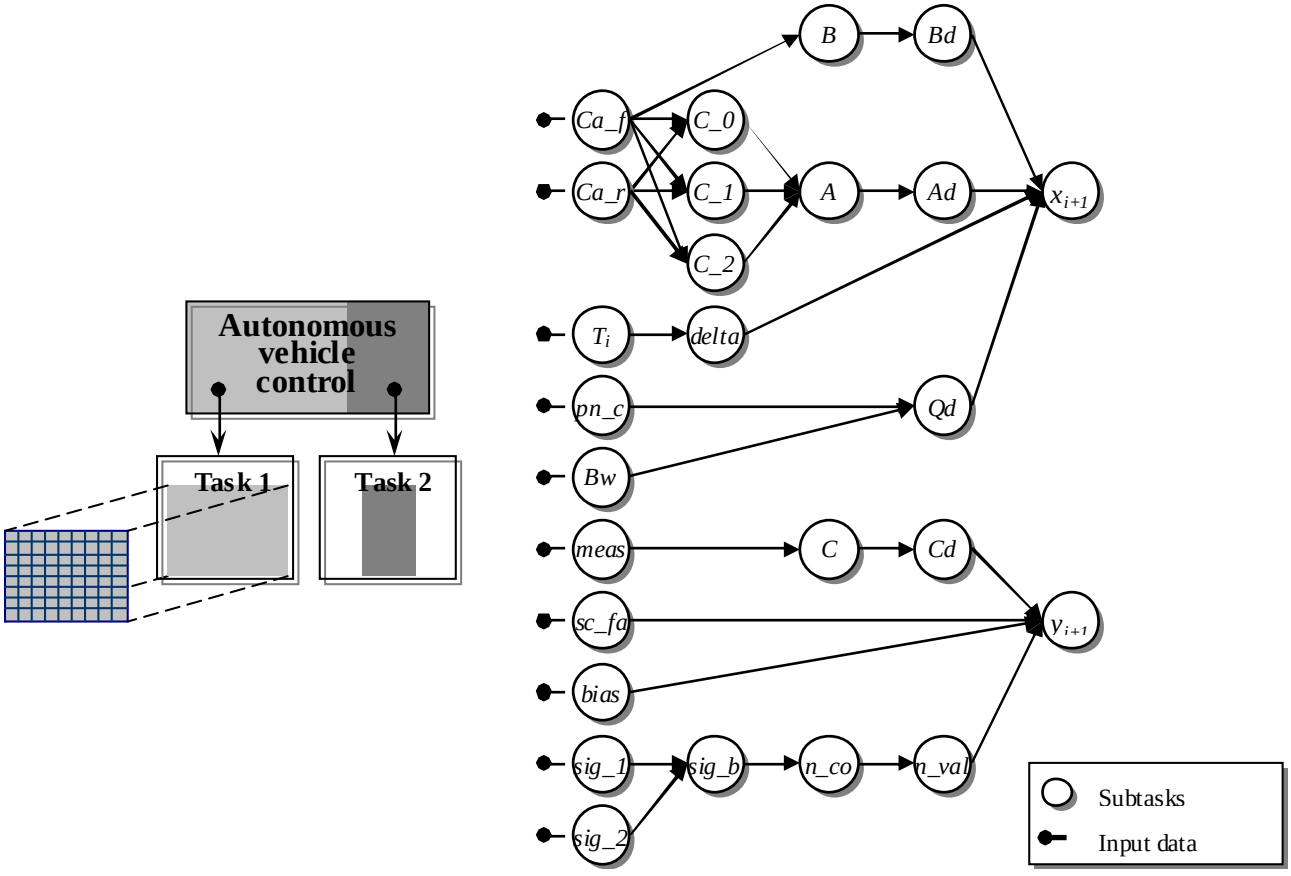

Figure 3. Decomposition diagram and subtasks graph for data decomposition of task 1

that represent the autonomous vehicle control we can conclude that the parallel fraction of code is 60%. According to Amdahl's law the speed up of the suggested method for an autonomous vehicle control is shown in figure 4.

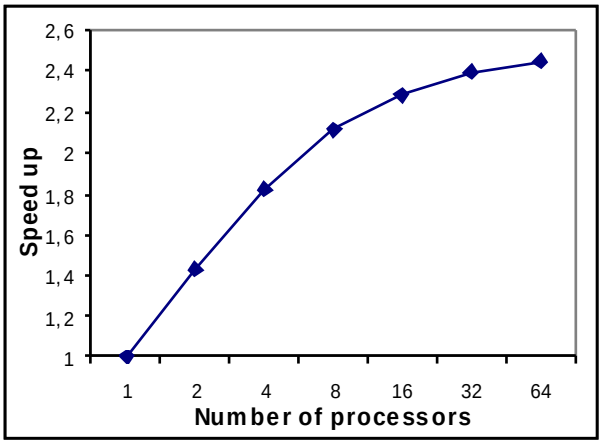

Figure 4. Speed up of the autonomous vehicle control method

The speed up reaches constant value when the number of the processors is 64. Amdahl's law provides a theoretical upper limit on parallel speedup assuming that there are no costs for communications. Nevertheless the achieved speed up is significant envisaging that Amdahl's law is fairly pessimistic.

4. Conclusions

The method for autonomous vehicle control has been proposed. Since this method has to be applied in real-time systems, it has been optimized in respect of two directions: linearization and parallel execution. The small angle approximation is used in order to remove the trigametric terms from the equations of motion. The parallel optimization shows increasing of the speed up according to number of processors due to parallel execution.

6. References

1. Rossetter, E., Swikes, J., Gerdes, J.: *A gentle nudge towards safety: Experimental validation of the potential field driver assistance system*. Proceedings of the American Control Conference, Denver, CO, U.S.A., June 2003, IEEE
2. Van Zanten, A., Erhardt, R., Pfaff, G., Kost, F., Hartmann, U., Ehret, T.: *Control aspects of the Bosch-VDC*. International Symposium on Advanced Vehicle Control, June 1996, p. 573–605
3. Gillespie, T.D.: *Fundamentals of Vehicle Dynamics*. Society of Automotive Engineers, Warrendale, PA, U.S.A., 1992
4. Pacejka, H., Bakker, E., Nyborg, L.: *Tyre Modeling for Use in Vehicle Dynamics Studies*. International Congress and Exposition, Detroit, MI, U.S.A., 1987
5. Milliken, W., Milliken, D.: *Race Car Vehicle Dynamics*. Society of Automotive Engineers, Warrendale, PA, U.S.A., 1995
6. Nakov, O., Petrova, D.: *Parallel programming* (*Theoretical and Applied Components*). Technical University of Sofia, Bulgaria, 2004

Received in March 2007, and revised form in June 2007